



[biblio.ugent.be](https://biblio.ugent.be)

The UGent Institutional Repository is the electronic archiving and dissemination platform for all UGent research publications. Ghent University has implemented a mandate stipulating that all academic publications of UGent researchers should be deposited and archived in this repository. Except for items where current copyright restrictions apply, these papers are available in Open Access.

This item is the archived peer-reviewed author-version of:

Automated extraction of the femoral shaft axis and its distal entry point from full and reduced 3D models

Sofie Van Cauter, Matthieu De Beule, Annemieke Van Haver, Peter Verdonk, Benedict Verheghe

In: Proceedings of the III ECCOMAS Thematic Conference on Computational Vision and Medical Image Processing: VipIMAGE 2011, p. 57-61

# Automated extraction of the femoral shaft axis and its distal entry point from full and reduced 3D models

S. Van Cauter<sup>1</sup>, M. De Beule<sup>1</sup>, A. Van Haver<sup>2,3</sup>, P. Verdonk<sup>4</sup> & B. Verheghe<sup>1</sup>

<sup>1</sup>*IBiTech-bioMMeda, Ghent University, Ghent, Belgium*

<sup>2</sup>*Engineering Department, Ghent University College, Ghent, Belgium*

<sup>3</sup>*Department of Mechanical Construction and Production, Ghent University, Ghent, Belgium*

<sup>4</sup>*Department of Orthopaedic Surgery, Ghent University Hospital, Ghent, Belgium*

**ABSTRACT:** During conventional total knee arthroplasty, the shaft or medial axis of the femur (FSA) is referenced by inserting an intramedullary rod (FIR), which is then used to position the femoral prosthesis. In this study, an automated technique, based on geometrical entity fitting, is presented for extracting the FSA and FIR from a 3D triangular surface mesh. The algorithms are tested using computed tomography scans of 50 cadaveric femurs. Furthermore, reduced models are processed and compared to the full models to study the feasibility of partially scanning the thigh. The mean deviations for two outer parts of 25% and a central part of 5% of the femoral length are smaller than 1 mm for the FSA and 0.3° and 0.5 mm for the orientation and entry point of a 150 mm long FIR. The automated methods could offer a valuable assistance to the surgeon for preoperative planning of FIR insertion.

**Keywords:** automated landmark extraction, femoral shaft axis, computed tomography, total knee arthroplasty

## 1 INTRODUCTION

The identification of anatomical reference parameters or landmarks, which are defined as prominent features of the body, is a well-established technique in orthopaedic surgery. A variety of morphological measurements and joint coordinate systems have been defined using such anatomical features. Landmarks are typically obtained by manual palpation of the subject or by virtual localization on a medical image. Manual analyses are, however, time-consuming and prone to observer variability and, consequently, an increasing amount of techniques for automated landmark extraction are being presented.

The femoral shaft (or anatomical) axis (FSA) is defined as the medial axis of the shaft (or diaphysis) of the femur and is usually straight in the frontal plane but curved in the sagittal plane. It is used as a reference parameter for positioning the femoral prosthesis in conventional total knee arthroplasty (TKA). The distal part of the axis is determined by manually inserting a metal rod into the medullary canal of the femur. The distal femur is then resected at a certain angle with respect to the intramedullary rod (FIR), aiming to put the femoral prosthesis orthogonally to

the mechanical axis. As it has been shown that the entry point location of the rod has an important influence on the alignment of the prosthesis (Reed 1997, Mihalko 2005), preoperatively determining this entry point could improve the alignment accuracy of TKA. In addition, the preoperative planning of the insertion of the FIR could be used to obtain a patient-specific distal femoral resection angle.

Different methods have been presented to automatically determine the FSA on 3D virtual femurs generated from computed tomography (CT) scans, such as distance-controlled thinning (Subburaj 2010), circle fitting (Mahaisavariya 2002) and cylinder fitting (Cerveri 2010). However, because of the radiation exposure involved in CT scanning, obtaining full femur scans is not feasible in patient treatment. A new method for computing the FSA, based on geometrical entity fitting, is therefore proposed, which can be applied to full and reduced models of the femur. Moreover, the orientation and entry point of a FIR with a length of 150 mm are computed from the distal part of the FSA. The femur is reduced in different ways and the analyses are compared to those of the full femur to determine the effect of the scanning reduction on the computed FSA and FIR.

## 2 MATERIALS & METHODS

To develop and test the algorithms, 50 CT scans of cadaveric femurs, with 0.79 x 0.79 mm pixel size and 0.63 mm slice increment, are processed. The bones are segmented and 3D triangular surface meshes are created using Mimics (Materialise NV, Leuven, Belgium). All further processing is performed automatically in pyFormex (<http://pyformex.org>), an open-source program under development at IBiTech-bioMMeda, providing a wide range of operations on surface meshes.

### 2.1 Preprocessing

Some preprocessing algorithms are applied to simplify the 3D mesh and to remove undesirable noise. First, the edge reduction algorithm of the GNU Triangulated Surface Library is applied, resulting in 66668 triangles for the full femur. The edge reduction is run with equal weights for volume, boundary and shape optimization (Lindstrom 1998). Next, the 3D model is smoothed with a volume-preserving low-pass filter (Taubin 1995), by applying 20 smoothing iterations with a scale factor of 0.5.

### 2.2 Standardised coordinate system

The femur, which is positioned randomly during CT scanning, is then oriented in a standardised way. The centre of gravity (C) and principal axes of inertia of the surface are calculated. These axes serve as a coarse approximation of the antero-posterior (AP), right-left (RL) and disto-proximal (DP) directions. Then, the RL axis is rotated parallel to the posterior condylar line (PCL) in the axial plane (Fig. 1). The PCL is calculated as the line connecting the most posterior points of the medial and lateral condyles. As the PCL depends on the AP direction, the coordinate system is iteratively rotated until the RL and PCL axes are parallel.

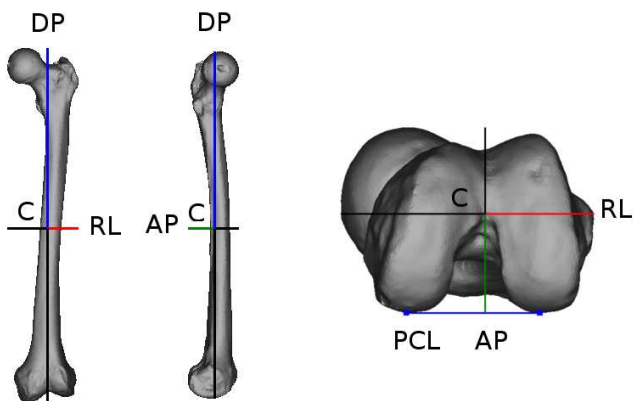


Figure 1. Standardised coordinate system: centre of gravity C and principal axes of inertia (RL,AP,DP) with RL rotated parallel to the posterior condylar line (PCL).

### 2.3 Reference parameters

The following step is to extract the femoral middle shaft axis (FMSA), which is defined as the straight medial axis of the middle diaphysis. This axis will be used to reduce the full models and thus simulate a partial scanning of the thigh. The FMSA is calculated by fitting an elliptic cylinder to a set of points that lies symmetrically around C and has a height that is equal to half of the femoral length along DP (Fig. 2-3 (a)). The axes of the standardised coordinate system are used as a starting estimate for the principal axes of the cylinder. The FMSA is defined by the longitudinal axis of the fitted cylinder.

The optimal position and sizes of the cylinder are computed by minimizing the sum of squares of the distances of the points to the cylinder. This minimization is done with the nonlinear Levenberg-Marquardt least-squares optimization routine of the SciPy library. For a general quadric, calculating the orthogonal Euclidean distance requires solving the following set of equations, which states that the line connecting the point  $x_p$  and its closest point  $x_c$  on the quadric  $Q(x)$  should be orthogonal to  $Q(x)$  in  $x_c$ :

$$\begin{cases} Q(x_c) = x_c A x_c^T + b x_c^T + c = 0 \\ x_p - x_c = t \nabla Q(x_c) = t(2x_c A + b) \end{cases} \quad (1)$$

The closest point  $x_c$  can be written as

$$x_c = (x_p - tb)(I + 2tA)^{-1} \quad (2)$$

Eliminating  $x_c$  from Equation 1 results in

$$\begin{aligned} (x_p - tb)(I + 2tA)^{-1} A (I + 2tA)^{-1} (x_p - tb)^T \\ + b(I + 2tA)^{-1} (x_p - tb)^T + c = 0 \end{aligned} \quad (3)$$

Calculating the orthogonal distances thus involves finding the roots of a (at most) sixth degree polynomial for every point. Moreover, these distances need to be computed for each iteration of the minimization algorithm. An approximate geometrical distance is therefore calculated for every point  $x_p$  by intersecting the quadric with the normal vector  $n$  of the surface mesh at  $x_p$ . This problem is described by Equation 4 and involves solving a second degree polynomial, as shown in Equation 5.

$$\begin{cases} Q(x_c) = x_c A x_c^T + b x_c^T + c = 0 \\ x_p - x_c = tn \end{cases} \quad (4)$$

$$(x_p - tn)A(x_p - tn)^T + b(x_p - tn)^T + c = 0 \quad (5)$$

To determine the FSA, which is defined as the curved medial axis of the diaphysis, a series of elliptic hyperboloids of one sheet are fitted to the shaft

(Fig. 2-3 (b)). The axes of the standardised coordinate system are used as an initial guess for the principal axes of the first (central) hyperboloid and each following hyperboloid is initialized by the principal axes of the previous one. All hyperboloids have a height between 5 and 10 mm, to provide enough surface points for the fitting procedure, while allowing to capture the curvedness of the shaft. The FSA is then represented by a cubic Bezier curve that is computed from the longitudinal axes of the fitted hyperboloids (Fig. 2-3 (c)). To find the distal and proximal endpoints of the curve, a stop criterion is implemented, stating that the radius change along the FSA should not be larger than 10%.

Finally, the orientation and entry point of a FIR with a length of 150 mm are computed by fitting a line to the distal part of the FSA and intersecting it with the distal surface of the femur (Fig. 2-3 (d)). An iterative process is used to fit the line to the part of the FSA lying 150 mm above the entry point.

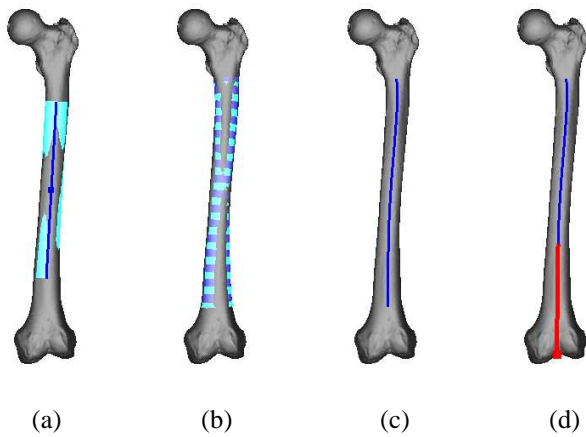


Figure 2. Reference parameters in the frontal plane: (a) femoral middle shaft cylinder and axis (FMSA); (b) femoral shaft hyperboloids; (c) femoral shaft axis (FSA); (d) femoral intramedullary rod (FIR).

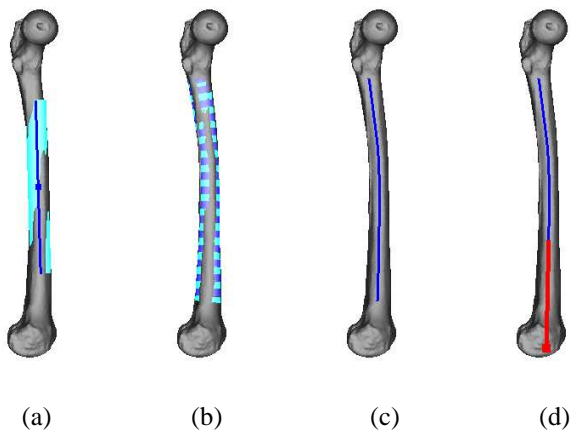


Figure 3. Reference parameters in the sagittal plane: (a) femoral middle shaft cylinder and axis (FMSA); (b) femoral shaft hyperboloids; (c) femoral shaft axis (FSA); (d) femoral intramedullary rod (FIR).

## 2.4 Comparison of full and reduced femur models

To simulate the effect of obtaining a partial scan of the patient's thigh, the femur model is reduced along its FMSA. Three reduction methods (distal, central and proximal part; distal and proximal part; distal part), two reduction amounts for the distal and proximal parts (30% and 25% of the femoral length) and two reduction amounts for the central part (10% and 5% of the femoral length) are studied. Figure 4 shows the different types of reductions with distal and proximal parts of 30% and a central part of 10% of the length. For the models consisting of more than one part, the FSA is interpolated to estimate the medial axis in the non-scanned regions.

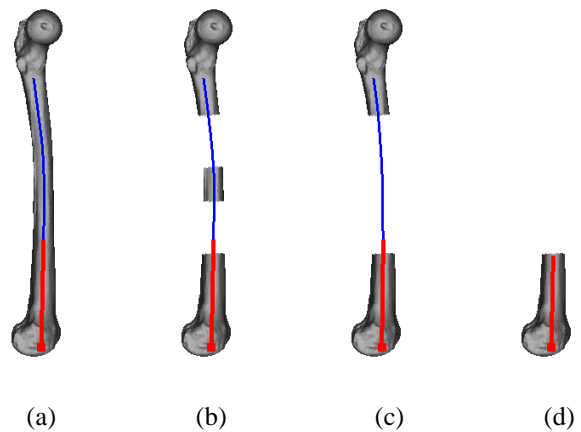


Figure 4. FSA computed on different types of models: (a) full model; (b) reduced model with distal, central and proximal part; (c) reduced model with distal and proximal part; (d) reduced model with distal part.

The FSA and FIR computed from the full and reduced models are compared using the following values: maximum orthogonal distance between the FSA (FSA-max); 3D distances between the distal/proximal endpoints of the FSA (FSA-DP/FSA-PP); absolute 3D angle between the axes of the FIR (FIR-A); 3D distance between the entry points of the FIR (FIR-EP).

## 3 RESULTS & DISCUSSION

Figure 5 shows the mean values and standard deviations for the 50 femur models for distal and proximal parts of 30% of the femoral length. The orthogonal distance between the FSA varies between  $0.10 \pm 0.07$  and  $2.21 \pm 0.50$  mm (FSA-max). It should be noticed that the smallest value is obtained for the reduction to one distal part, because no interpolation can be used here to estimate the FSA in the non-scanned regions. The largest value is found for the reduction to a distal and proximal part. The FSA of these models has a highly larger deviation from the FSA of the full model compared to the first two cases. Removing the central part forces the curve to

interpolate directly between the outer parts, thereby misestimating the curvature of the bone. The 3D distances between the endpoints (FSA-DP and FSA-PP) are rather similar for the different cases and have a maximum value of  $0.40 \pm 0.36$  mm. The values for the FIR orientation and entry point are between  $0.14 \pm 0.09$  and  $0.94 \pm 0.45^\circ$  (FIR-A) and between  $0.23 \pm 0.16$  and  $1.43 \pm 0.65$  mm (FIR-EP). The best results are obtained for the models with a central part of 10%, while a large increase is shown for the models without central part. Overall, the models with central parts of 10% and 5% have similar mean values and standard deviations.

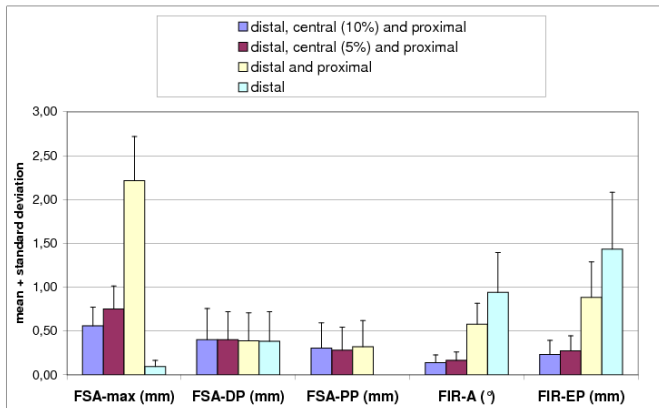


Figure 5. Comparison of the analyses of the full and reduced femur models for distal and proximal parts of 30% of the length.

The results for distal and proximal parts of 25% of the femoral length are displayed in Figure 6. The same observations as in Figure 5 can be made between the different reduction cases. Compared to the outer parts of 30%, larger values are shown. Good results for all parameters are obtained for the central part of 5%, with mean deviations from the full models smaller than 1 mm (FSA-max), 0.5 mm (FSA-DP and FSA-PP),  $0.3^\circ$  (FIR-A) and 0.5 mm (FIR-EP). The maximum values are smaller than 2 mm, 3.1 mm,  $1.3^\circ$  and 2.1 mm.

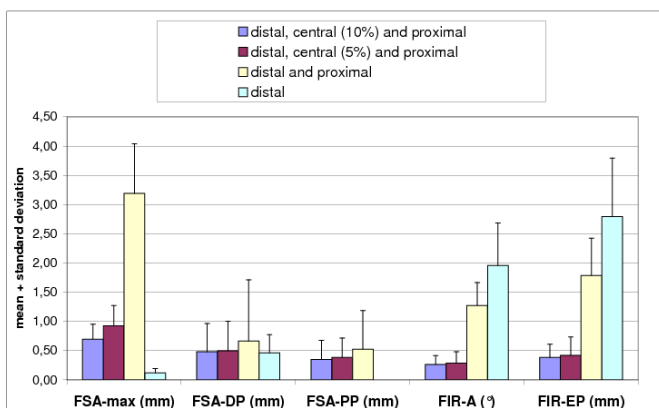


Figure 6. Comparison of the analyses of the full and reduced femur models for distal and proximal parts of 25% of the length.

It was found that reducing the outer parts to 20% results in too few hyperboloids in these regions and incorrect endpoints for the FSA.

The results of this study indicate that scanning 55% of the thigh gives precise values for the FSA and a 150 mm long FIR. To correctly capture the curvedness of the shaft (and thus of the FSA), it is recommended to scan a distal, central and proximal part of the thigh. It is also shown that the orientation of the FIR largely depends on the curvedness of the FSA, as considerably higher deviations from the full model are obtained when the central part is omitted.

The automated extraction of the FIR orientation and entry point may contribute to a faster and more objective planning of TKA. However, some limitations of the current study should be mentioned. Mesh simplification and smoothing was applied on the 3D models, but the effect of various parameters for these preprocessing operations should be investigated. Also, the insertion of intramedullary rods with different lengths should be studied. In particular, larger rods may inhibit a complete insertion because the medullary canal is curved, and it might thus be important to take into account the canal width. Further work is being carried out to evaluate the computed values by comparison with a set of manually identified parameters and to extract the mechanical axis of the femur to find a patient-specific distal resection angle for TKA procedures. The proposed methods could then allow for automatic planning of FIR insertion and distal femoral resection preoperatively, offering a valuable assistance to the surgeon.

#### 4 CONCLUSIONS

An automated method for computing the FSA was developed and tested on 50 femur models. The orientation and entry point of a FIR used for TKA alignment was derived from the distal part of the FSA. It was shown that the FSA and FIR can be determined with high precision by scanning two outer parts and a central part of the thigh. The automated method could offer a valuable assistance to the surgeon for TKA procedures by preoperatively planning FIR insertion.

#### 5 ACKNOWLEDGEMENT

The authors gratefully acknowledge Dr. Emmanuel Audenaert (Department of Orthopaedic Surgery, Ghent University Hospital) and the Department of Experimental Anatomy of the Vrije Universiteit Brussel for providing the CT scans.

## REFERENCES

- Cerveri P, Marchente M, Bartels W, Corten K, Simon JP, Manzotti A. 2010. Automated method for computing the morphological and clinical parameters of the proximal femur using heuristic modeling techniques. *Ann Biomed Eng* 38(5):1752-1766.
- Lindstrom P, Turk G. 1998. Fast and memory efficient polygonal simplification. *Proceedings of IEEE Visualization '98*. Research Triangle Park, North Carolina, 18-23 October, p. 279-286.
- Mahaisavariya B, Sitthiseripratip K, Tongdee T, Bohez EL, Vander Sloten J, Oris P. 2002. Morphological study of the proximal femur: a new method of geometrical assessment using 3-dimensional reverse engineering. *Med Eng Phys* 24(9):617-622.
- Mihalko WM, Boyle J, Clark LD, Krackow KA. 2005. The variability of intramedullary alignment of the femoral component during total knee arthroplasty. *J Arthroplasty* 20(1):25-28.
- Reed SC, Gollish J. 1997. The accuracy of femoral intramedullary guides in total knee arthroplasty. *J Arthroplasty* 12(6):677-682.
- Subburaj K, Ravi B, Agarwal M. 2010. Computer-aided methods for assessing lower limb deformities in orthopaedic surgery planning. *Comput Med Imaging Graph* 34(4):277-288.
- Taubin G. 1995. A signal processing approach to fair surface design. Paper presented at: SIGGRAPH '95. *Proceedings of the 22nd Annual Conference on Computer Graphics*. Los Angeles, CA, USA, 6-11 August, p. 351-358.